GENERALIZED TARGETING PARAMETERS FOR THE GUIDANCE OF AEROSPACE VEHICLES

by

RICHARD MARVIN McCRANEY

A THESIS

Submitted in partial fulfillment of the requirements
for the degree of Master of Science in Engineering
in the Huntsville Graduate Programs in the
Graduate School of the University of Alabama

UNIVERSITY, ALABAMA

1968

ACKNOWLEDGEMENTS

The author wishes to express his appreciation to Dr. T. R. Beal for his helpful suggestions and comments in the preparation of this thesis, to Mrs. Barbara Morrow for typing the final copy as well as several preliminary drafts, and to his wife for her patience and understanding.

BIOGRAPHICAL SKETCH

Richard Marvin McCraney was born August 16, 1942, at Pensacola, Florida, to Mary Edna (McConnell) McCraney and the late Wilson Grady McCraney. After completing his secondary education in Pensacola, Florida in 1960, he received a B.S. degree in Aerospace Engineering from Auburn University at Auburn, Alabama, in March 1965. He was accepted to the Graduate School of the University of Alabama in 1965, and has taken courses at the University of Alabama in Huntsville. He has been employed by NASA at Langley Research Center in Virginia and is presently employed by Northrop Space Laboratories in Huntsville. He is married to Marilyn (Hughes) McCraney.

TABLE OF CONTENTS

LIST OF ILLUSTRATIONS

DEFINITION OF SYMBOLS

Symbol	Definition
a	Nominal semimajor axis of target orbit
AZ	Launch azimuth
$\vec{D}_N$	Unit vector through the intersection of the nominal target orbit plane and the equatorial plane
e	Eccentricity of transfer conic
e_N	Nominal eccentricity of transfer conic
$2E$	Twice nominal energy of target orbit
$\vec{F}$	Vector through intersection of target orbit plane and the equatorial plane (line of nodes)
$\vec{F}_p$	Vector perpendicular to $\vec{F}$ in the target orbit plane
g	Instantaneous gravity
G_T	Terminal gravity
h	Nominal angular momentum of target orbit
i	Inclination of orbit
$\vec{M}$	Negative unit aim vector
$\vec{N}$	Normal to nominal target orbit plane
$\vec{N}_{PC}$	Normal to perturbed conic plane
$\vec{N}_{PO}$	Normal to instantaneous parking orbit
P	Semilatus rectum of target conic
P_N	Nominal semilatus rectum of target conic
$\vec{P}_1$	Vector perpendicular to radius vector in parking orbit
$\vec{R}_i$	Instantaneous radius vector

DEFINITION OF SYMBOLS (Continued)

Symbol	Definition
$\vec{R}_{NT}$	Terminal radius vector for the nominal conic
$\vec{R}_T$	Terminal radius vector
$\vec{R}_{ig}$	Reignition vector in Earth parking orbit
$\vec{R}_p$	Vector perpendicular to terminal radius vector in nominal target orbit plane
$\vec{R}'$	Unit terminal radius vector for the nominal conic
$\vec{R}'_i$	Unit instantaneous radius vector
$\vec{S}$	Nodal vector through intersection of parking orbit and transfer conic plane
$\vec{S}_L$	Vector perpendicular to perigee vector
$\vec{S}_p$	Perigee vector
T	Time to cutoff of burn phase
$\vec{V}_i$	Instantaneous velocity vector
$\vec{V}_T$	Terminal velocity vector
$\vec{V}_{NT}$	Terminal velocity vector for the nominal conic
$\vec{V}_g$	Velocity to be gained by the vehicle
α_D	Angle from the perigee vector to the descending nodal vector
α_{TS}	Angle between the $\vec{S}$ and $\vec{M}$ vectors
β	Constant angle defining the location of the $\vec{S}$ vector with respect to the radius vector in the ignition plane at reignition
θ_N	Descending nodal angle of target orbit
θ_T	Desired flight path angle
σ	True anomaly of negative aim vector
ϕ	True anomaly of terminal radius vector
ϕ_L	Geodetic latitude of launch site

DEFINITION OF SYMBOLS (Concluded)

Symbol	Definition
ϕ_T	Range angle measured from descending node
$\tilde{\chi}$	Direction of thrust vector if velocity only is enforced
χ_p	Pitch steering command
χ_y	Yaw steering command
$\vec{\Omega}_x$	Vector through intersection of launch meridian and equatorial plane
$\vec{\Omega}_y$	Vector through South Pole
$\vec{\Omega}_z$	Vector pointing East in the equatorial plane

ABSTRACT

This thesis presents the development of the equations necessary to compute the targeting parameters for the iterative guidance mode for all types of space missions. A brief introduction to the iterative guidance mode is presented as well as the derivation and explanation of the necessary equations to compute the targeting parameters. Experimental verification of the equations is also included.

CHAPTER I

INTRODUCTION

This thesis presents the development of the equations necessary to compute the targeting parameters (radius, velocity, etc.) for the iterative guidance mode. The iterative guidance mode is an inertial type guidance scheme that is used to compute the guidance commands for the Saturn launch vehicles. The equations are developed so that they may be applied towards any type space missions; these include circular Earth orbital insertion missions, direct ascent missions, and lunar or planetary injection missions from an Earth parking orbit.

The lunar or planetary injection missions from an Earth parking orbit make use of a rather new concept called the hypersurface. The term hypersurface simply refers to a surface of conics which contains the same conic parameters and fulfills the mission requirements. This concept is discussed in detail later in the thesis. The introduction, itself, is directed towards a general discussion of guidance.

Fundamental to the problem of the motion of a space vehicle from one point of the Earth's surface or one point of space to another, is the development of a suitable guidance and control system to accomplish the guidance functions. Such a system will consist of the following: sensors for measuring various vehicle dynamical variables such as acceleration, velocity, and position; a suitable computation and control system such as a digital and/or analog computer whose function is to process the information

provided by the system's sensors; and the necessary propulsion control units whose function is to develop and apply forces and moments to the vehicle in the manner directed by the computer's outputs.

As an example, the computer may be called upon to determine where the vehicle is located in space. This may be done by carrying out suitable computations based on inputs from the acceleration measuring devices. The computer will "know" the desired destination of the vehicle and this information, coupled with knowledge of the vehicle's present position and some desired steering philosophy, will lead to the determination of the necessary signals sent to the control units.

The guidance and control system may be operative continuously throughout the flight of the space vehicle as would be the case for low thrust interplanetary vehicles. On the other hand, it may only be operative over small fractions of time during the vehicle's flight such as in the guidance of ballistic rockets or ballistic interplanetary scientific research vehicles.

Guidance theory in general is concerned with the development of a two-point boundary value problem. For example, assume that the equations of motion of a space vehicle are of the form

$$\frac{dx_i}{dt} = f_i(x_1,\ldots,x_m,\ u(t),t) \qquad i=1,\ldots,m$$

where the x_i are the state variables, such as position and velocity coordinates, and $u(t)$ is the guidance (control) function to be chosen, such as the angle of the rocket thrust relative to an inertial reference. The initial condition $x(t_o)$ is given, and it is desired that, at the final time T, certain coordinates $x_i(T)$ take on prescribed values. If there exists a $u(t)$ which accomplishes this task, there will, in

general, be many such functions. Thus, one seeks an optimal $u_o(t)$ which satisfies the end conditions while minimizing some performance index.

Guidance can be defined as the task of calculating and executing corrective maneuvers which will cause the vehicle to achieve desired end conditions, given the state of the vehicle. The state of the vehicle consists of the position and velocity as well as the longitudinal acceleration and the gravitational acceleration.

The choice of a guidance mode requires the consideration of many factors. Some of these factors are:

1. Optimality - Given that there is a performance index to be minimized, for example propellant expenditure, how does the obtained value of the performance compare to the theoretical minimum?
2. Accuracy - Given that approximations are introduced into the derivation and mechanization of the guidance equations, what are the resulting errors in the desired terminal conditions? These errors can be classified according to:
   a. Approximations errors - due to analytical approximations introduced into the derivation of the guidance equations.
   b. Computer errors - due to the inaccuracies of the numerical methods used to implement the guidance equations (truncation and roundoff).
   c. Mechanization errors - due to the inability of the vehicle to physically respond to the guidance commands.
3. Region of Applicability - What is the range of perturbations which can be treated accurately by the guidance mode?

4. Preflight preparation - What is the cost in time and money of preflight preparation of the guidance equations? In particular, how long does it take to prepare the guidance system to accomplish a given mission?
5. Computer factors - What are the real time on-board and/or Earth-based computer requirements? In particular, how much storage space is required, what is the length of the computing cycle for each iteration of the guidance equations, and how complex must the computer be?
6. Flexibility - What are the types of missions which the guidance mode can perform and how well can it adapt to changes in the mission?
7. Growth potential - What is the potential applicability of the guidance mode to future missions?

One type of guidance mode that has widespread use in aerospace work is inertial guidance. This is a system of directing a vehicle and determining its location without reference to any fixed points outside the system. This is the only navigation system that is entirely self-contained and does not need to depend, once it is launched, on any exterior source of orientation. Instead, it relies mainly on Newton's laws of motion. Inertial refers to the property of a mass tending to remain at rest or in uniform motion in the absence of applied forces. This first law of Newton, making the conditions of rest and uniform motion identical, rules out the possibility of direct determination of velocity by inertial means. The second law, by identifying a force with a change of velocity of a mass

$$F = d(MV)/dt$$

gives the opportunity of sensing such a change and of obtaining velocity by integration. The third law, by equating action and reaction, suggests the use of an accelerometer to detect this change in velocity.

This is the type of guidance system used on the Saturn launch vehicles. It is an inertial type guidance system and uses accelerometers to perform its measurements. The next chapter discusses the iterative guidance mode.

CHAPTER II

DISCUSSION OF THE ITERATIVE GUIDANCE MODE

The iterative guidance mode is an inertial system mode in that the only inputs required after liftoff are available from the onboard navigation system. It computes steering commands as a function of the state of the vehicle (velocity, position, gravitational acceleration, and longitudinal accelerations) and the desired terminal conditions.

The iterative guidance scheme is also path adaptive in that it produces steering commands in pitch and yaw which enable the vehicle to obtain desired terminal conditions with maximum payload. During the burn phase, this scheme computes continuously the ideal thrust direction that will satisfy the mission in the best possible manner. The need for a path adaptive mode such as this is necessary due to the development of multi-stage rockets with the capability of injecting large payloads into lunar and planetary orbits.

Two earlier type guidance modes, the "delta minimum" and "velocity to be gained", are not satisfactory for these missions. Under the "delta minimum" mode, steering is based on comparing the locally measured values of certain state variables with those on a precalculated standard trajectory, that is known to cause fulfillment of the mission. The nulling of the differences in these variables is then the basis of the steering philosophy for the vehicle. Under the "velocity to be gained" mode, the flight is not forced back to a standard trajectory. An approximation of the vector difference between the locally measured velocity vector

and one, that if assumed instantaneously would produce mission fulfillment, is computed. Nulling the vector difference between the velocities then secures the mission.

Both of these modes are satisfactory for the purposes for which they were developed. The "delta minimum" mode is not satisfactory for multistage space vehicles because the assumption of staying close to a standard trajectory is violated by the altered trajectory necessary for sufficient engine-out performance. Satisfactory performance is also a problem in the "velocity to be gained" mode since the various missions for large space vehicles do not fit directly into a locally desired velocity vector formulation.

The iterative guidance scheme updates the guidance commands each guidance cycle, using the updated state of the vehicle. This path adaptive guidance mode retains its optimization properties under all types of vehicle perturbations without any loss in accuracy at cutoff. This includes large thrust deviations, engine-out cases, weight uncertainties, specific impulse changes, variations in initial altitude or velocity, and any other reasonable perturbations. It can be applied to any mission for which cutoff conditions can be defined such as Earth orbital insertion, near-Earth elliptic orbits, lunar injection from Earth orbits, and planetary injection from Earth orbits.

Calculus of variations (references 6 and 7) shows that the optimum thrust direction in a vacuum over a flat earth with a constant gravitational field, constant thrust, and constant specific impulse is

$$\tan\chi = \frac{a+bt}{c+dt}$$

where a, b, c, and d are constants depending on the boundary conditions. If only a velocity end condition is enforced, it can be shown that a constant thrust direction is the optimum steering law (references 6 and 10). The thrust direction can be shown by the following geometric construction:

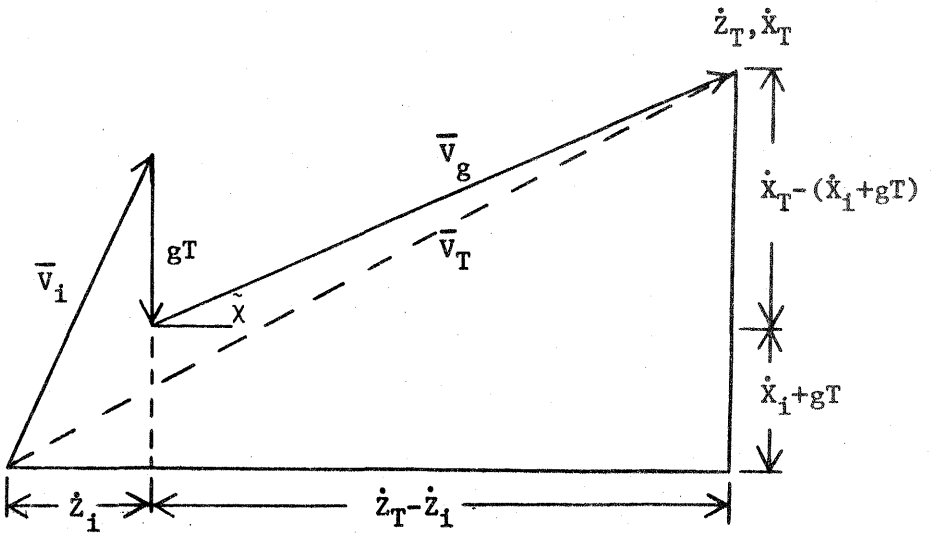

Figure 1. GEOMETRY OF THE THRUST DIRECTION FOR A VELOCITY CONSTRAINT

$$\tan\tilde{\chi} = \frac{\dot{X}_T - (\dot{X}_i + gT)}{\dot{Z}_T - \dot{Z}_i}$$

where

T = Time to cutoff

$\bar{V}_i$ = Initial velocity vector

$\dot{Z}_i$ = Initial velocity in Z direction

$\dot{X}_i$ = Initial velocity in X direction

gT = Velocity loss due to gravity

$\bar{V}_T$ = Cutoff velocity vector

$\dot{Z}_T$ = Cutoff velocity in Z direction

$\dot{X}_T$ = Cutoff velocity in X direction

$\overline{V}_g$ = Velocity to be gained by the vehicle

$\dot{\chi}$ = Direction of thrust vector if velocity only is enforced.

If velocity and altitude are enforced, a first order expansion of the calculus of variations law becomes

$$\chi = a + bt \ .$$

The iterative guidance mode computes the thrust direction (with velocity and altitude enforced) using a steering law of this form

$$\chi = \tilde{\chi} - K_1 + K_2 \, \Delta t \ ,$$

where K_1 and K_2 are subject to the conditions that the velocity constraint enforced by $\tilde{\chi}$ is not violated. Each evaluation cycle updates $\tilde{\chi}$, K_1, and K_2, using the current state variables and vehicle characteristics. Δt is the time lapse since the last guidance evaluation cycle. Using a steering law of this form for χ_p and χ_y, the guidance system directs the vehicle to its desired terminal conditions. A three-dimensional view of the χ_p and χ_y angles is shown in Figure 2.

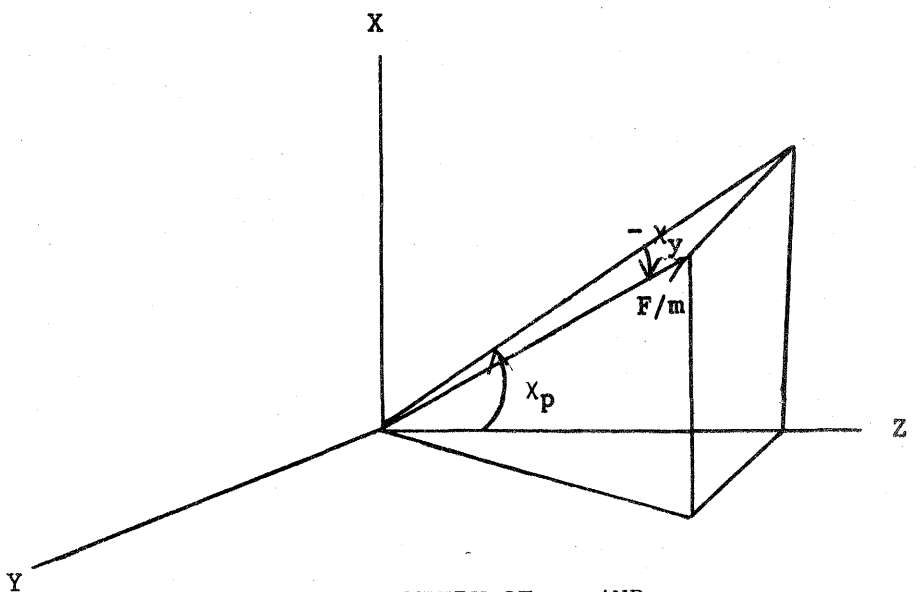

Figure 2. GEOMETRY OF χ_p AND χ_y

This is the basic principle of the iterative guidance mode steering philosophy. The χ_p and χ_y angles that orient the thrust vector are computed using the form of an expression from calculus of variations. Most of the factors discussed in the introduction that should be considered in the choice of a guidance mode are fulfilled by the iterative guidance mode: it does calculate its guidance commands in an optimum manner; its accuracy is extremely reliable; its performance is very satisfactory under any reasonable perturbation; it does not require an excessive amount of preflight preparation; the amount of computer space is well within the limits necessary; and it is extremely flexible in that it can be used for any mission in which cutoff conditions can be defined. As stated previously, the purpose of this thesis is to present the equations that can be used to compute these cutoff conditions for any type of space mission. Literature on the complete development of the iterative guidance mode is readily available (references 6, 10, and 11).

CHAPTER III

DEVELOPMENT OF GENERALIZED TARGETING EQUATIONS

Five quantities specify the terminal (cutoff) conditions for the iterative guidance scheme:

(1) Radial distance from the center of the Earth

(2) Velocity magnitude

(3) Path angle against the local horizontal

(4) Inclination of the orbit plane to the equator

(5) Descending node of the orbit plane relative to the launch meridian.

These are the five quantities any targeting routine must supply to the iterative guidance mode. The purpose of the equations derived in this section is to determine these five quantities for all types of space missions. The types of missions can be broken into the following three groups:

(A) Circular Earth Orbital Insertion

(B) Direct Ascent

(C) Lunar or Planetary Injection from an Earth Parking Orbit.

The equations can be programmed into a targeting subroutine and the proper option selected to determine which equations are used.

The following values are assumed known:

AZ - Launch azimuth

ϕ_L - Geodetic latitude of the launch site

ϕ_T - Range angle

β - Angle from reignition in the Earth parking orbit to the intersection of the transfer conic and parking orbit plane (only needed for missions requiring lunar or planetary injection from an Earth parking orbit).

σ - True anomaly of the negative aim vector (only needed for cases β is used)

α_{TS} - Angle between the $\vec{S}$ and $\vec{M}$ vectors (also only needed when β is used)

$\vec{R}_i$ - Instantaneous vehicle position vector

$\vec{V}_i$ - Instantaneous vehicle velocity vector

$\vec{R}_{NT}$ - Terminal radius vector for the nominal trajectory

$\vec{V}_{NT}$ - Terminal velocity vector for the nominal trajectory.

The coordinate system used in the derivations is an Earth center plumbline coordinate system with the X-axis vertical, the Z-axis along the launch azimuth, and the Y-axis completing the right hand system. The basic geometry of this system with several important angles included is illustrated in Figure 3.

The parameters that are assumed known are obtained from a nominal trajectory for a given mission. Regardless of the type mission, several parameters are computed using the same equations. These parameters are the basic conic parameters and the angles depending only on launch conditions.

The magnitude of the nominal terminal (cutoff) radius and velocity is

$$R_{NT} = |\vec{R}_{NT}| \tag{1}$$

and

$$V_{NT} = |\vec{V}_{NT}|. \tag{2}$$

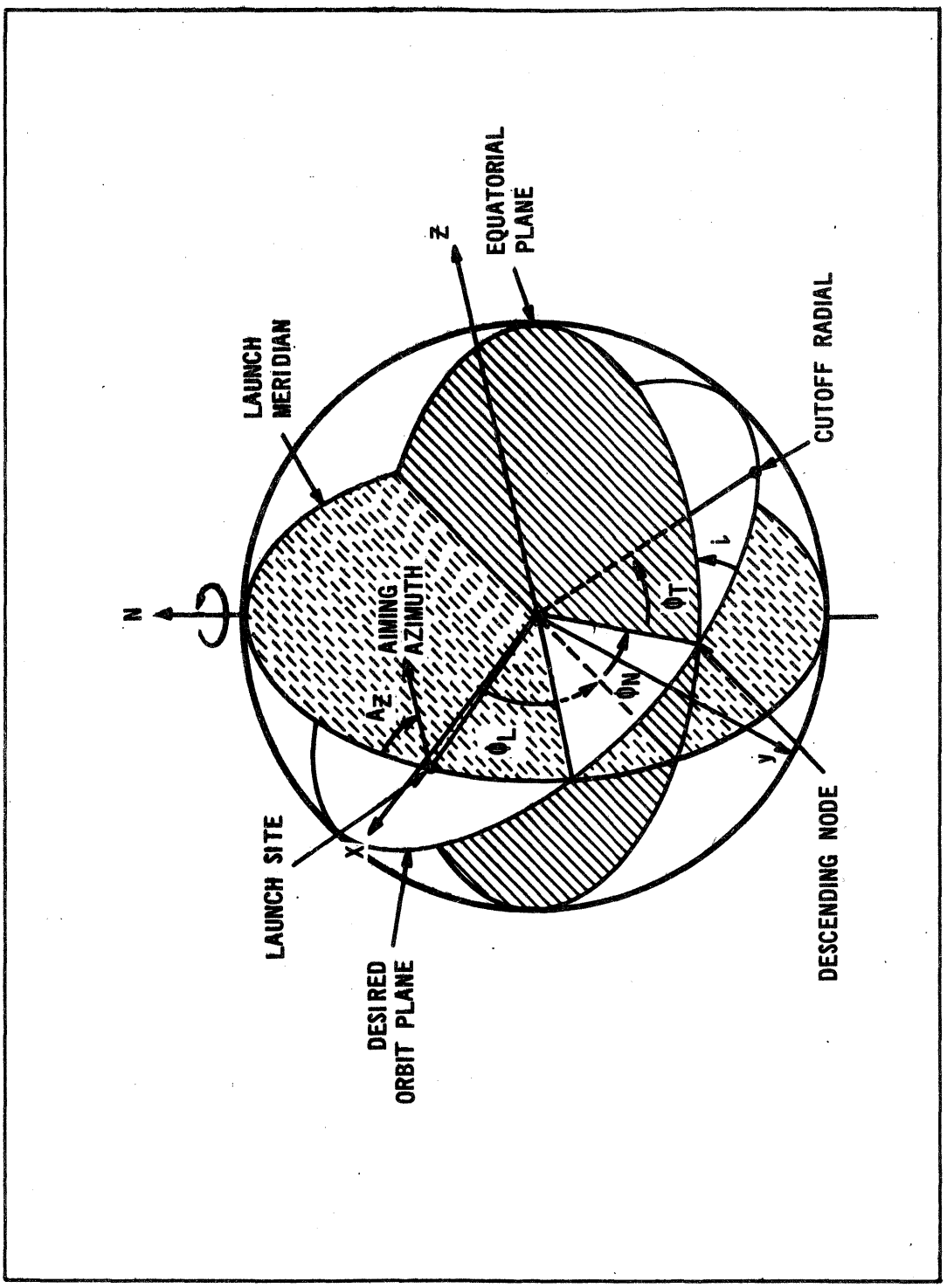

Figure 3. FLIGHT GEOMETRY

A normal vector to the nominal cutoff plane is obtained by crossing the unit radius and velocity vectors

$$\vec{N} = \frac{\vec{R}_{NT} \times \vec{V}_{NT}}{|\vec{R}_{NT} \times \vec{V}_{NT}|} \quad . \tag{3}$$

The semilatus rectum is found by

$$P = h^2/\mu$$

$$P = \frac{R^2V^2(1-\cos^2\theta)}{\mu}$$

$$P_N = \frac{R_{NT}^2V_{NT}^2-(\vec{R}_{NT}\cdot\vec{V}_{NT})^2}{\mu} \tag{4}$$

where

P_N is the nominal semilatus rectum, and

μ is the Earth gravitational constant.

The angular momentum is

$$h = \sqrt{\mu P} \tag{5}$$

and twice the energy is found by

$$2E = V_{NT}^2 - \frac{2\mu}{R_{NT}} \quad . \tag{6}$$

The semi-major axis is

$$a = -\mu/2E \quad . \tag{7}$$

Here, a check on the sign is necessary. If the conic is hyperbolic ($2E > 0$), the sign must be changed to ensure "a" remains positive. If the conic is elliptical, eccentricity is computed by

$$e_N = \sqrt{1 - P_N/a} \quad ; \tag{8}$$

if the conic is hyperbolic, e_N must be computed by

$$e_N = \sqrt{P_N/a + 1} \quad . \tag{9}$$

Three vectors that can be obtained by using the launch azimuth and geodetic latitude of the launch site are necessary to determine the node and inclination of the desired orbit. These vectors are

(1) A vector through the launch meridian in the equatorial plane

(2) A vector pointing due East in the equatorial plane

(3) A vector through the South Pole, called the omega vector of the Earth.

These three vectors are obtained by rotating the plumbline Earth centered coordinates by the launch azimuth and the geodetic latitude of the launch site. The first rotation is through the aiming azimuth about the X-axis.

$$\begin{bmatrix} X' \\ Y' \\ Z' \end{bmatrix} = \begin{bmatrix} 1 & 0 & 0 \\ 0 & \sin AZ & -\cos AZ \\ 0 & \cos AZ & \sin AZ \end{bmatrix} \begin{bmatrix} X \\ Y \\ Z \end{bmatrix}$$

This forms an Earth-centered X', Y', Z' system with the X'-axis vertical, Z'-axis pointing East, and Y' normal to the X'-Z' plane. This system is then rotated through the angle ϕ_L (latitude of the launch site) about the Z'-axis.

$$\begin{bmatrix} X'' \\ Y'' \\ Z'' \end{bmatrix} = \begin{bmatrix} \cos\phi_L & \sin\phi_L & 0 \\ -\sin\phi_L & \cos\phi_L & 0 \\ 0 & 0 & 1 \end{bmatrix} \begin{bmatrix} X' \\ Y' \\ Z' \end{bmatrix} \tag{10}$$

This forms an X", Y", Z" system with the origin at the center of the Earth, where X" is passing through the intersection of the launch meridian and the equatorial plane, Z" is pointing East and lying in the equatorial plane, and Y" is passing through the South Pole. This yields three unit vectors as follows

$$\begin{bmatrix} \cos\phi_L & \sin\phi_L & 0 \\ -\sin\phi_L & \cos\phi_L & 0 \\ 0 & 0 & 1 \end{bmatrix} \times \begin{bmatrix} 1 & 0 & 0 \\ 0 & \sin AZ & -\cos AZ \\ 0 & \cos AZ & \sin AZ \end{bmatrix} =$$

$$\begin{bmatrix} \cos\phi_L & \sin\phi_L \sin AZ & -\sin\phi_L \cos AZ \\ -\sin\phi_L & \cos\phi_L \sin AZ & -\cos\phi_L \cos AZ \\ 0 & \cos AZ & \sin AZ \end{bmatrix} \qquad (11)$$

where the rows of the rotated matrix represent $\vec{\Omega}_x$, $\vec{\Omega}_y$, $\vec{\Omega}_z$. These three vectors can be written in the X, Y, Z system using the three unit vectors i, j, and k which are directed along the X, Y, and Z axis, respectively.

$\vec{\Omega}_x = \cos\phi_L \vec{i} + \sin\phi_L \sin AZ \vec{j} - \sin\phi_L \cos AZ \vec{k}$, and is a unit vector through the intersection of the launch meridian and equatorial plane.

$\vec{\Omega}_y = -\sin\phi_L \vec{i} + \cos\phi_L \sin AZ \vec{j} - \cos\phi_L \cos AZ \vec{k}$, and is a unit vector through the South Pole.

$\vec{\Omega}_z = \cos AZ \vec{j} + \sin AZ \vec{k}$, and is a unit vector pointing East in the equatorial plane.

Another vector necessary is the vector through the intersection of the nominal target orbit plane and equatorial plane (line of nodes).

This vector is obtained by crossing the normal vector of the target orbit and a vector through the North Pole $(-\vec{\Omega}_y)$

$$\vec{D}_N = \vec{N} \times (-\vec{\Omega}_y) \ . \qquad (12)$$

This completes the equations necessary to determine the basic conic parameters of the target orbit and several vectors necessary for later calculations. In summary, the following have been determined:

R_{NT} - Nominal terminal radius

V_{NT} - Nominal terminal velocity

$\vec{N}$ - Normal vector to the nominal target plane

P_N - Semilatus rectum of the nominal conic

h - Angular momentum of the nominal conic

2E - Twice the energy of the nominal conic

a - Semi-major axis of the nominal conic

e_N - Eccentricity of the nominal conic

$\vec{\Omega}_x$ - Unit vector through the intersection of the launch meridian and equatorial plane

$\vec{\Omega}_y$ - Unit vector through the South Pole

$\vec{\Omega}_z$ - Unit vector pointing due East in the equatorial plane

and

$\vec{D}_N$ - Unit vector through the intersection of the nominal target orbit and the equatorial plane.

A. Circular Earth Orbital Insertion Missions

Circular parking orbits are always obtained by specifying fixed end conditions. The term fixed end conditions means that the terminal radius, velocity,

and flight path angle are prespecified constants and do not change during the burn phase of the mission. For a particular mission the terminal R_T, V_T, and θ_T are the cutoff conditions of a nominal trajectory that satisfy all mission constraints. These terminal conditions will specify certain conic parameters (the parameters previously given). Since the iterative guidance scheme does not enforce the range angle, any vehicle performance perturbation will cause a rotation of the conic. However, if the path angle has been specified as zero, then a circular parking orbit will result and the only effect a rotation has, is to change the time to reach the terminal conditions. Therefore, the R_{NT} and V_{NT} previously determined will be the terminal radius and velocity for a circular orbit. Three other parameters still must be determined (θ_T, i, and θ_N). The flight path angle is determined as

$$\theta_T = \sin^{-1} \frac{\vec{R}_{NT} \cdot \vec{V}_{NT}}{R_{NT}\, V_{NT}} . \tag{13}$$

It is easily seen that the inclination is

$$i = \cos^{-1} (-\vec{\Omega}_y \cdot \vec{N}) , \tag{14}$$

where $-\vec{\Omega}_y$ is the omega vector of the Earth through the North Pole and $\vec{N}$ is the normal vector to the target orbit.

The descending node is found by

$$\theta_N = \tan^{-1} \frac{\vec{D}_N \cdot \vec{\Omega}_z}{\vec{D}_N \cdot \vec{\Omega}_x} \tag{15}$$

which is the angle from the launch meridian to the intersection of the target orbit plane and equatorial plane.

One other parameter that can be easily obtained is the terminal gravity which is

$$G_T = - \mu/R_T^2 \ . \tag{16}$$

This completes the equations necessary to be used for Earth orbital insertion missions that are circular. The five quantities that the targeting subroutine must supply to the iterative guidance mode have been determined.

In summary, the five quantities are:

(1) $R_T = R_{NT}$

(2) $V_T = V_{NT}$

(3) $\theta_T = \sin^{-1} \dfrac{\vec{R}_{NT} \cdot \vec{V}_{NT}}{R_{NT} \, V_{NT}}$

(4) $i = \cos^{-1} (-\vec{\Omega}_y \cdot \vec{N})$

(5) $\theta_N = \tan^{-1} \dfrac{(\vec{D}_N \cdot \vec{\Omega}_z)}{(\vec{D}_N \cdot \vec{\Omega}_x)}$

B. Direct Ascent Missions

The direct ascent type missions include elliptical Earth orbital insertion missions and launching directly, without an intermediate parking orbit, into a lunar or planetary transfer conic. These missions can be either fixed or variable end condition. By variable end condition it is meant that R_T, V_T, and θ_T change during the burning phase but the orientation, shape, and size of the desired conic remain constant. One note of importance here is that the inclination and node are calculated from the nominal conditions but the true anomaly of cutoff varies. This

is to be distinguished from the case using the hypersurface (presented next) where the orientation of the conic is allowed to vary. To use variable end conditions, an angle not mentioned before is needed. This is α_D, the angle from the perigee vector to the descending nodal vector. The range angle, ϕ_T, is measured from the descending nodal vector to the terminal radius vector; therefore, the sum of α_D and ϕ_T gives the true anomaly of the terminal radius vector. Hence, by varying the range angle each integration cycle R_T, V_T, and θ_T can be varied.

The perigee vector is illustrated in the following sketch,

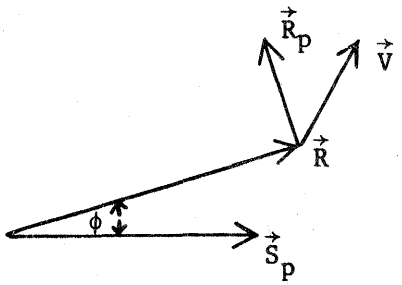

where $\vec{S}_p$ is the perigee vector, $\vec{R}$ is the terminal radius vector, $\vec{V}$ is the terminal velocity vector, $\vec{R}_p$ is the unit vector perpendicular to the radius vector in the plane of $\vec{R}$ and $\vec{V}$, and ϕ is the true anomaly of the terminal radius vector. Let

$$\vec{R}' = \frac{\vec{R}}{|\vec{R}|}$$

and

$$\vec{R}_p = \frac{\vec{R}\times\vec{V}}{|\vec{R}\times\vec{V}|} \times \frac{\vec{R}}{|\vec{R}|} \quad .$$

The sketch shows the perigee vector can be defined as

$$\vec{S}_p = \vec{R}' \cos\phi - \vec{R}_p \sin\phi \quad . \qquad (A)$$

It is necessary to express the perigee vector in terms of variables already determined.

$$\vec{R}_p = \frac{1}{h} [(\vec{R}x\vec{V})x\vec{R}] \frac{1}{R} \qquad (B)$$

where

$$h = |\vec{R} \times \vec{V}| \ .$$

Also, by using

$$(\vec{A}x\vec{B})x\vec{C} = (\vec{A}\cdot\vec{C})\vec{B} - (\vec{B}\cdot\vec{C})\vec{A}$$

one obtains

$$(\vec{R}x\vec{V})x\vec{R} = (\vec{R}\cdot\vec{R})\vec{V} - (\vec{V}\cdot\vec{R})\vec{R} = R^2\vec{V} - \dot{R}R\vec{R} = R(R\vec{V} - \dot{R}\vec{R}) \qquad (C)$$

where

$$\dot{R} = V \cos\theta$$

Substituting (C) into (B) yields

$$\vec{R}_p = \frac{1}{h} R(R\vec{V} - \dot{R}\vec{R}) \frac{1}{R} = \frac{1}{h} [R\vec{V} - \dot{R}\vec{R}] \qquad (D)$$

To determine $\cos\phi$ and $\sin\phi$ one recalls that

$$R = \frac{P}{1 + e\cos\phi} \ .$$

Therefore

$$\cos\phi = \frac{P-R}{Re} \ . \qquad (E)$$

Now

$$\frac{dR}{dt} = (1 + e\cos\phi)^{-2} (e\sin\phi)P \frac{d\phi}{dt} \ .$$

Using

$$R^2 \frac{d\phi}{dt} = R^2\dot{\phi} = h$$

yields

$$\frac{d\phi}{dt} = \frac{h}{R^2} = \frac{\sqrt{P\mu}}{R^2} \ .$$

Therefore

$$\frac{dR}{dt} = (1 + e\cos\phi)^{-2}\, e\sin\phi\, P\, \frac{\sqrt{P\mu}}{R^2}$$

$$= (1 + e\cos\phi)^{-2}\, e\sin\phi\, P\, \frac{\sqrt{P\mu}}{P^2}\, (1 + e\cos\phi)^2$$

$$= e\sin\phi\, \frac{\sqrt{P\mu}}{P}$$

$$\dot{R} = e\sin\phi\, \sqrt{\mu/P}$$

or

$$\sin\phi = \frac{\dot{R}}{e}\, \frac{1}{\sqrt{\mu/P}}$$

$$= \frac{\dot{R}}{e}\, (P/\mu)^{1/2} . \qquad (F)$$

Substituting (D), (E), and (F) into (A) yields

$$\vec{S}_p = \cos\phi\, R' - \sin\phi\, \vec{R}_p$$

$$= \frac{P-R}{Re}\, \left(\frac{\vec{R}}{R}\right) - \frac{\dot{R}}{e}\, (P/\mu)^{1/2}\, \left(\frac{1}{h}\, (R\vec{V} - \dot{R}\vec{R})\right)$$

$$= \left[\frac{P-R}{eR^2} + \frac{\dot{R}^2}{eh}\, (P/\mu)^{1/2}\right]\, \vec{R} - \left[\frac{\dot{R}R}{eh}\, (P/\mu)^{1/2}\right]\, \vec{V} \qquad (17)$$

which defines the perigee vector in variables already obtained except for $\dot{R}$; $\dot{R}$ is simply found by

$$\frac{\vec{R}\cdot\vec{V}}{R} = V\cos\theta = \dot{R} .$$

The $\vec{R}$ and $\vec{V}$ vectors in equation (17) are actually the $\vec{R}_{NT}$ and $\vec{V}_{NT}$ vectors that are assumed known.

The inclination and descending node are obtained using the same equations that are in the circular Earth orbit insertion case. That is

$$i = \cos^{-1}\, (-\vec{\Omega}_y \cdot \vec{N}) \qquad (18)$$

and

$$\theta_N = \tan^{-1} \frac{(\vec{\Omega}_z \cdot \vec{D}_N)}{(\vec{\Omega}_x \cdot \vec{D}_N)} \tag{19}$$

In order to determine the angle α_D, a vector perpendicular to the perigee vector is found by

$$\vec{S}_L = \vec{N} \times \vec{S}_p \tag{20}$$

and α_D is then

$$\alpha_D = \tan^{-1} \frac{(\vec{D}_N \cdot \vec{S}_L)}{(\vec{D}_N \cdot \vec{S}_p)} \tag{21}$$

which is the angle from perigee to the descending node. The true anomaly of the cutoff point is

$$\phi = \phi_T + \alpha_D \tag{22}$$

where ϕ_T is the range angle measured from the descending node to the cutoff point. R_T, V_T, and θ_T are expressed as a function of the true anomaly as follows:

$$R_T = \frac{P_N}{1 + e \cos\phi} \tag{23}$$

and

$$\begin{aligned} V_T^2 &= \frac{2\mu}{R_T} - \frac{\mu}{a} \\ &= \frac{2\mu}{P_N}(1 + e\cos\phi) - \frac{\mu(1 - e^2)}{P_N} \\ V_T &= \left(\frac{\mu}{P_N}\right)^{1/2} (1 + 2e\cos\phi + e^2)^{1/2} \end{aligned} \tag{24}$$

and θ_T is obtained by

$$h^2 = R^2V^2 \sin^2\theta = \mu P_N$$

hence

$$\sin^2\theta = \frac{\mu P_N}{R^2 V^2}$$

$$\sin^2\theta = \frac{\mu P_N}{P_N^2 V^2}\,(1 + e\cos\phi)^2$$

$$\sin^2\theta = \frac{\mu(1 + e\cos\phi)^2}{P_N \mu\left(\frac{2}{R} - \frac{1}{a}\right)}$$

$$= \frac{(1 + e\cos\phi)^2}{\frac{P_N}{a}\left(\frac{2a}{R} - 1\right)}$$

$$= \frac{(1 + e\cos\phi)^2}{\frac{a(1-e^2)}{a}\left(\frac{2a\,(1+e\cos\phi)}{a(1-e^2)} - 1\right)}$$

$$= \frac{(1 + e\cos\phi)^2\,(1 - e^2)}{(1-e^2)(1 + 2e\cos\phi + e^2)}$$

therefore

$$\sin\theta = \frac{1 + e\cos\phi}{(1 + 2e\cos\phi + e^2)^{1/2}} \quad . \qquad \text{(A)}$$

The cosine of the angle is

$$\cos\theta = (1 - \sin^2\theta)^{1/2}$$

$$= \left[1 - \frac{(1 + e\cos\phi)^2}{(1 + 2e\cos\phi + e^2)}\right]^{1/2}$$

$$= \left[\frac{e^2 \sin^2\phi}{1 + 2e\cos\phi + e^2}\right]^{1/2} \quad . \qquad \text{(C)}$$

Now

$$\tan\theta = \frac{\sin\theta}{\cos\theta}$$

which gives θ with respect to the local vertical; therefore, to obtain θ with respect to the horizontal, the inverse is used

$$\tan \theta_T = \frac{\cos\theta}{\sin\theta}$$

$$\tan \theta_T = \frac{\dfrac{e \sin\phi}{(1 + 2e \cos\phi + e^2)^{1/2}}}{\dfrac{1 + e \cos\phi}{(1 + 2e \cos\phi + e^2)^{1/2}}}$$

$$= \frac{e \sin\phi}{1 + e \cos\phi}$$

which gives

$$\theta_T = \tan^{-1} \frac{e \sin\phi}{1 + e \cos\phi} \qquad (25)$$

This completes the equations necessary to compute the five targeting parameters for a direct ascent type mission. The terminal radius, velocity, and flight path angle have been determined as a function of the range angle. This allows these values to be updated (variable end conditions) depending on the updated range angle. But, the orientation of the target conic (inclination and node) has been determined using the nominal $\vec{R}_{NT}$ and $\vec{V}_{NT}$ hence the orientation remains fixed.

In summary, the five quantities for the Direct Ascent Type missions are:

(1) $$R_T = \frac{P_N}{1 + e \cos\phi}$$

(2) $$V_T = \left(\frac{\mu}{P_N}\right)^{1/2} (1 + 2e \cos\phi + e^2)^{1/2}$$

(3) $$\theta_T = \tan^{-1} \frac{e \sin\phi}{1 + e \cos\phi}$$

$$(4) \quad i = \cos^{-1} (-\vec{\Omega}_y \cdot \vec{N})$$

$$(5) \quad \theta_N = \tan^{-1} \frac{(\vec{\Omega}_z \cdot \vec{D}_N)}{(\vec{\Omega}_x \cdot \vec{D}_N)}$$

C. Lunar or Planetary Injection from an Earth Parking Orbit

The lunar or planetary injection missions from an Earth parking orbit use the hypersurface to compute the targeting parameters. As previously stated, hypersurface refers to a surface of conics containing the same conic parameters which fulfill the mission requirements. The difference in using the hypersurface and simply flying to variable end conditions is that the orientation of the conic may be changed. This is equivalent to a slight (but allowable) relaxing of the constraint on the direction of the target velocity vector.

The hypersurface formulation allows the correct geometry to be established so that a desired condition can be satisfied in both time and space. Figure 4 shows the geometry for a lunar mission. The ignition point in an Earth parking orbit and the resulting cutoff on a translunar injection ellipse are indicated as well as the lunar hyperbola. If an aim point is taken as the sphere of influence of the Moon (50 hr. aim point), this simplified conic can be used to generate a surface of ellipses all of which will satisfy the basic constraints of the mission.

An attempt to build a guidance scheme based on the determination of the injection points on an exact cutoff hypersurface would be an extremely complex task. This would necessitate taking into account the n-body problem and the oblateness effects of the Earth, Moon, and any other bodies pertaining to a certain mission. However, the exact cutoff hypersurface can be simplified to the two-body problem with minimum losses

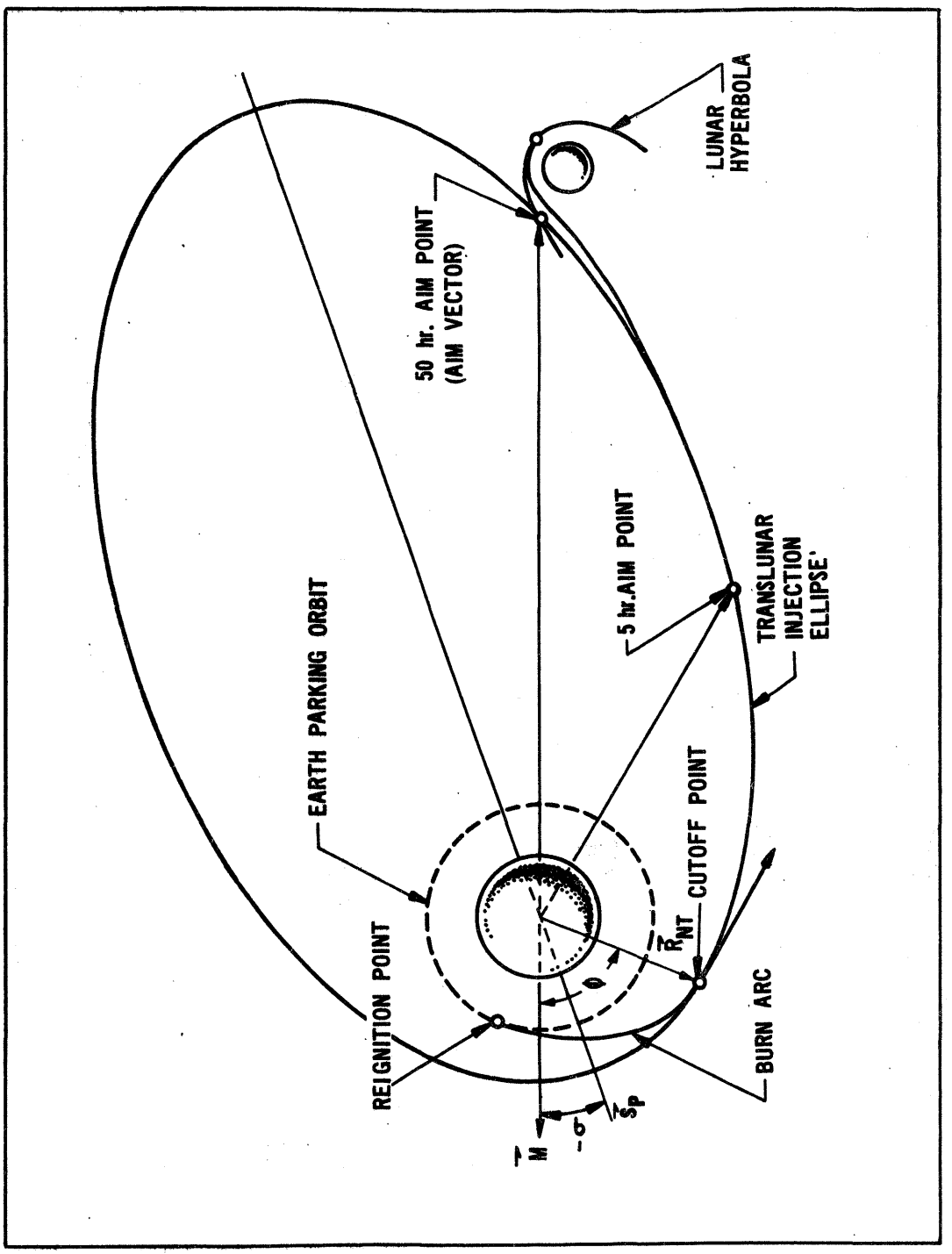

Figure 4. GEOMETRY OF LUNAR CONIC

in payload and in accuracy at the end conditions through the proper choice of a simplified cutoff hypersurface geometry. This simplified cutoff hypersurface can be solved in closed form by Keplerian mechanics. The knowledge of cutoff criterion allows the target injection guidance problem to be reduced to the achievement of points on the simplified cutoff hypersurface rather than the achievement of the desired conditions at cutoff.

The exact cutoff hypersurface would represent the solution of the n-body problem for the translunar or interplanetary ballistic free flight; however, the perturbing effects of the Earth's oblateness and of the Sun's, Moon's, and other planets gravitational influence do not significantly perturb the actual ballistic trajectory of the vehicle from that assuming only a spherical Earth. It is therefore reasonable to assume that a determination of ellipses which replace the actual ballistic trajectories will give very close approximations to the actual ballistic trajectory.

To force every set of perturbations in waiting orbit to inject at points on the nominal transfer ellipse would result in appreciable loss of payload. The loss of payload can be reduced considerably by rotating the nominal transfer ellipse in space about the aim vector so that an optimum maneuver will be performed during the injection burn. This will place the vehicle on one of the conics shown in Figure 5.

This yields the surface of conics with the same conic parameters that will fulfill the mission requirements. The equations necessary to define the hypersurface and the necessary logic to determine which of these conics should be used are now presented. Recalling that one variable

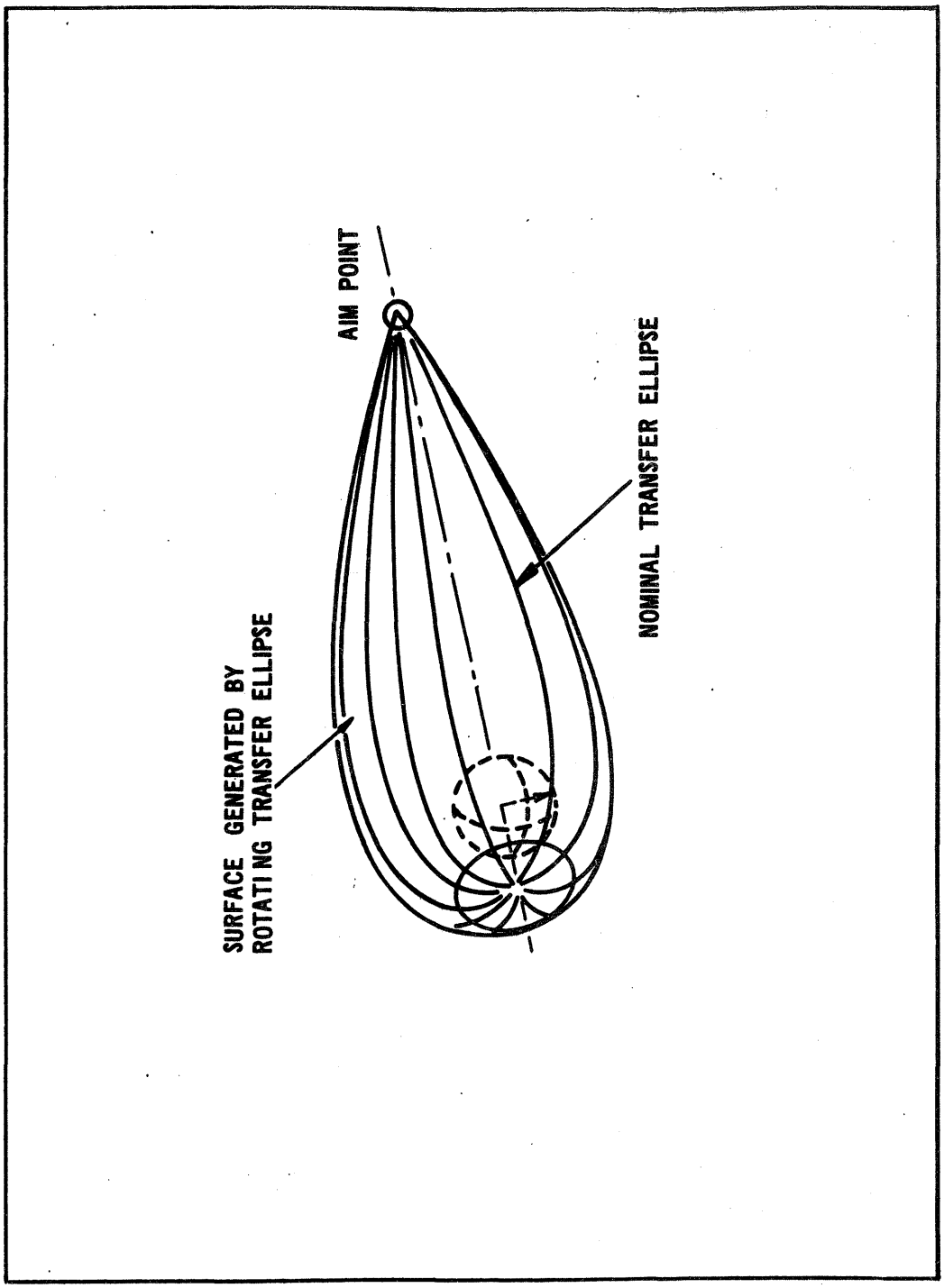

Figure 5. GEOMETRY OF THE HYPERSURFACE

that is assumed known is σ, the true anomaly of the negative aim vector, one may determine the negative aim vector as follows. The normal to the radius vector in the nominal cutoff plane is

$$\vec{R}_p = \vec{N} \times \vec{R}_{NT}. \tag{26}$$

The true anomaly of the nominal cutoff vector is

$$\Phi = \cos^{-1} \frac{1}{e_N} \left(\frac{P_N}{R_{NT}} - 1\right) \tag{27}$$

which allows the unit negative aim vector to be obtained by

$$\vec{M} = \frac{1}{R_{NT}} \left[\vec{R}_{NT} \cos (\sigma-\phi) + \vec{R}_p \sin (\sigma-\phi)\right]. \tag{28}$$

This is the negative of the aim vector $(\vec{M})$ shown in Figure 4. The derivation of this equation is obvious from the following sketch.

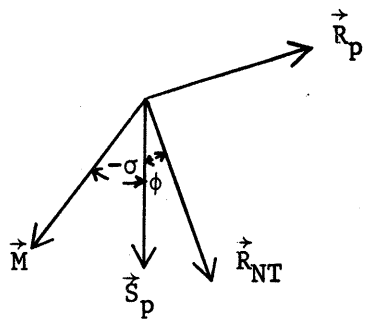

Reviewing the basic conic parameter equations developed earlier and equation (28) will reveal why target arrival errors are small when cutoff is approximated by simple two-body conic equations. The desired cutoff energy and eccentricity are computed using the cutoff conditions of the nominal. The negative aim vector is computed in the nominal cutoff plane using the true anomaly of the nominal cutoff vector and the input true anomaly of the negative aim vector. Although the actual cutoff plane as determined by the hypersurface will depend upon parking

orbit perturbations, the hypersurface equations will insure that the injection point (cutoff) defined by the hypersurface equations will be near the injection point of the nominal. This means that both ballistic trajectories will experience almost the same gravitational perturbations.

Now that the negative aim vector has been determined, it is necessary to determine which one of the conics of the hypersurface should be used. This is found by using the proper reignition criteria in the parking orbit. The angles α_{TS} and β are two empirically determined angles used in the reignition test and both are assumed known. If the orbital trace is projected on a plane above the negative aim vector, the nominal parking orbit will appear as an ellipse on that plane. A parking orbit that contains the negative aim vector will appear as a straight line as shown in Figure 6. The intersection of the Earth parking orbit and the surface of the target conics that passes through the aim point is denoted by the empirically determined angle α_{TS} (line of nodes). It has been determined that when the parking orbit position is projected ahead by a fixed empirically determined angle β and the angle α_{TS} is satisfied by a test, the optimum ignition time and the best target injection plane from a standpoint of maximum payload are determined. The normal to the instantaneous parking orbit is

$$\vec{N}_{PO} = \frac{\vec{R}_i \times \vec{V}_i}{|\vec{R}_i \times \vec{V}_i|} \tag{29}$$

The normal to the radius vector is found by using the unit radius vector, R_i',

$$\vec{P}_1 = \vec{N}_{PO} \times \vec{R}_i' \tag{30}$$

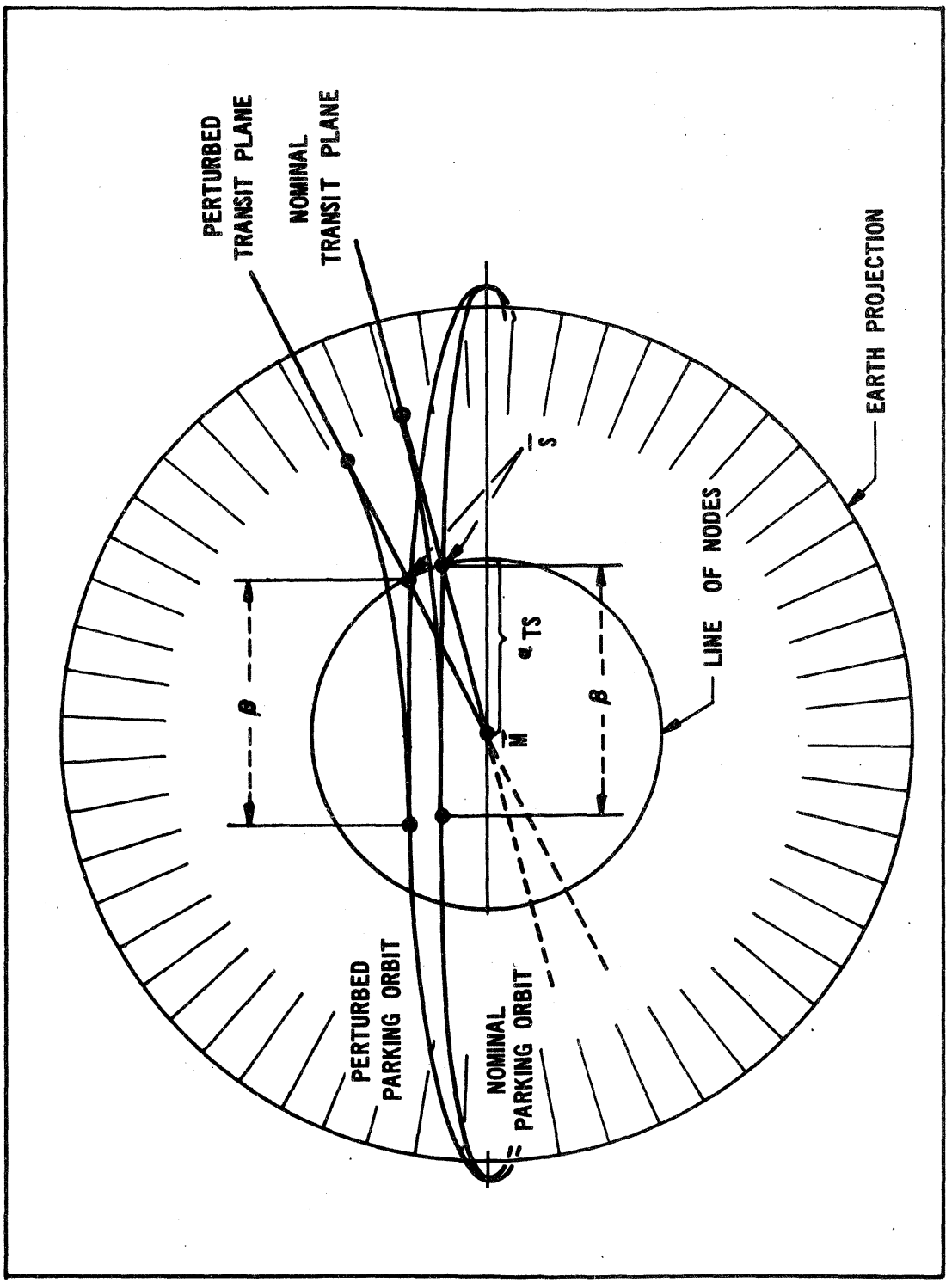

Figure 6. LUNAR OR PLANETARY INJECTION PLANE

The instantaneous position vector is then projected ahead by the angle β to determine the $\vec{S}$ vector

$$\vec{S} = \vec{R}_i' \cos\beta + \vec{P}_1 \sin\beta \ . \tag{31}$$

This vector, $\vec{S}$, is defined as the nodal vector of the parking orbit plane and injection plane when the reignition criteria is satisfied. The reignition test is then performed by

$$\vec{S} \cdot \vec{M} \leq \cos \alpha_{TS} \ . \tag{32}$$

When this test is satisfied, reignition occurs. These two angles β and α_{TS} will hold for any perturbed parking orbit that is within the flight performance reserves of the vehicle. Therefore, by observing Figure 6 it is clearly shown that any out-of-plane perturbation is taken care of by the reignition criteria and the injection plane is determined. Figure 7 shows a different perspective of the parking orbit and injection plane. This shows that the vectors $\vec{M}$ and $\vec{S}$ completely define the transfer plane.

At this point the transfer plane has been determined; hence, the specific properties such as node and inclination are now needed. The normal to the now perturbed transfer conic plane is

$$\vec{N}_{PC} = \frac{\vec{S} \times \vec{M}}{|\vec{S} \times \vec{M}|} \ . \tag{33}$$

The unit nodal vector of this plane is

$$\vec{F} = \frac{(\vec{S} \times \vec{M}) \times \vec{\Omega}_y}{|(\vec{S} \times \vec{M}) \times \vec{\Omega}_y|} \ . \tag{34}$$

The perigee vector is then easily found by

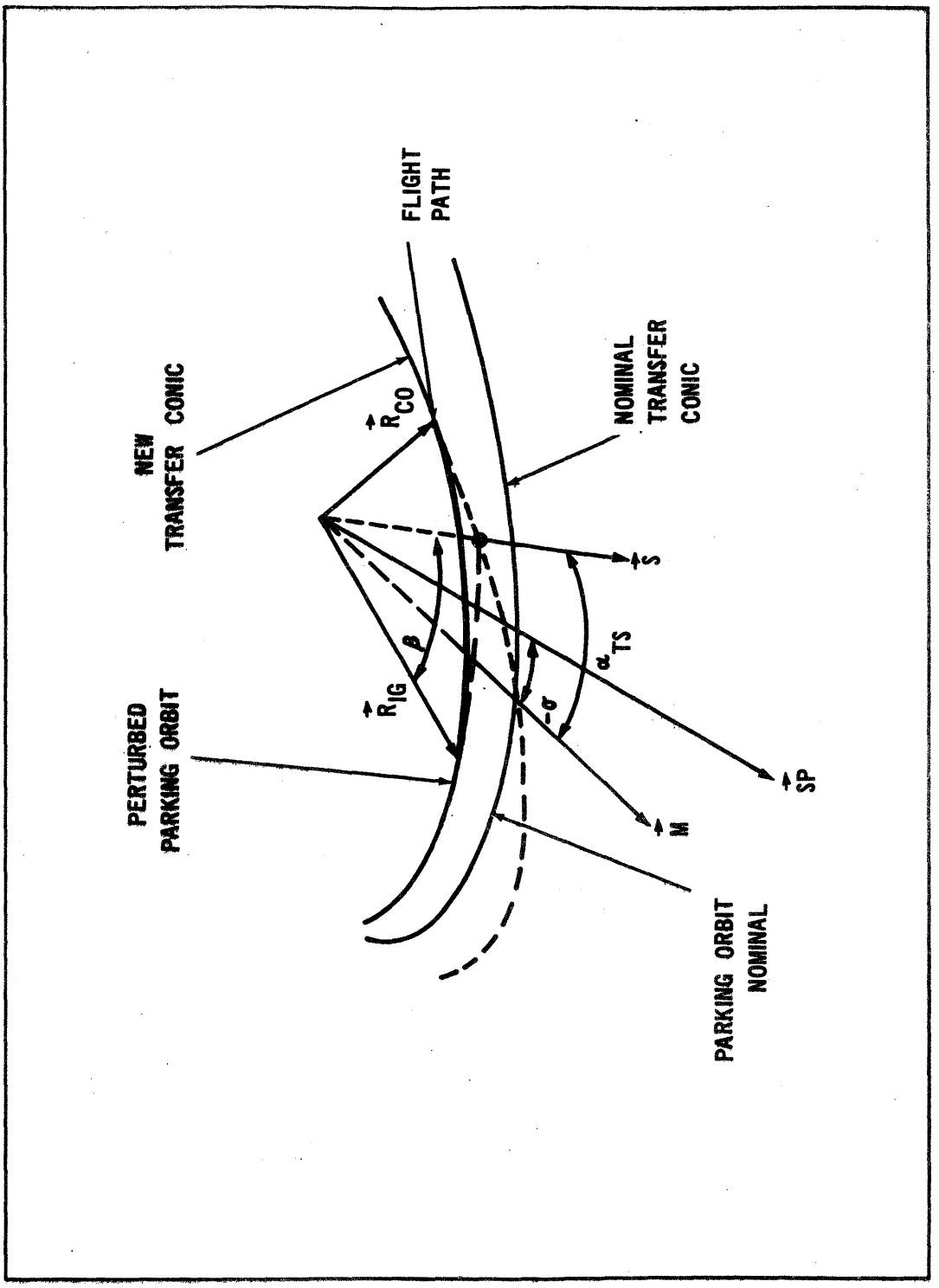

Figure 7. ORIENTATION OF PERTURBED TRANSFER CONIC

$$\vec{S}_p = \cos\sigma\ (\vec{M}) - \sin\sigma\ (-\vec{N}_{PC} \times \vec{M}) \qquad (35)$$

where σ is the true anomaly of the negative aim vector and $\vec{M}$ is the unit negative aim vector. $-\vec{N}_{PC} \times \vec{M}$ is perpendicular to the negative aim vector as shown in the following sketch

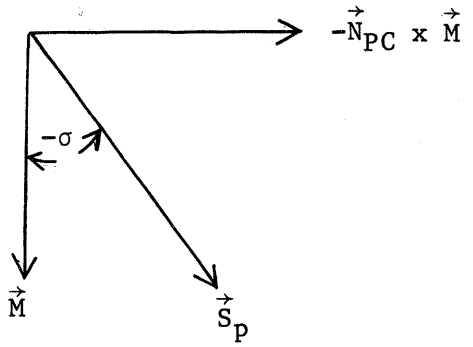

A vector perpendicular to the nodal vector is

$$\vec{F}_p = \vec{N}_{PC} \times \vec{F}.$$

The angle from perigee to the descending node, α_D, is found by

$$\alpha_D = \tan^{-1} \frac{(\vec{S}_p \cdot \vec{F}_p)}{(\vec{S}_p \cdot \vec{F})} . \qquad (36)$$

The inclination and node are then determined by

$$i = \cos^{-1} (\vec{\Omega}_y \cdot \vec{N}_{PC}) \qquad (37)$$

and

$$\theta_N = \tan^{-1} \frac{(\vec{\Omega}_z \cdot \vec{F})}{(\vec{\Omega}_x \cdot \vec{F})} .$$

At this point the equations to determine the orientation of the conic have been derived as well as the equation for α_D. This takes care of any out-of-plane perturbations, but the possibility of in-plane perturbations must also be considered. If the cutoff conic were invariant when a

parking orbit altitude variation occurred, large payload losses would result. Small payload losses can be maintained by varying the eccentricity of the cutoff ellipse so that the altitude gained by the nominal profiles is enforced. Figure 8 illustrates the corrections to be made to a nominal transfer ellipse for in-plane perturbations of the Earth parking orbit to maintain optimality of the power flight trajectory profile. This can be accomplished by changing the eccentricity by the ratio of the reignition radius magnitude of the perturbed parking orbit to the reignition radius magnitude of the nominal parking orbit

$$e = (R_i/R_{NPO})(e_N - 1) + 1 \tag{38}$$

where R_i is the instantaneous radius and R_{NPO} is the nominal parking orbit radius. The semilatus rectum can then be recalculated using the new eccentricity

$$P = (\mu/2E)(1 - e^2) \tag{39}$$

As in the direct ascent type mission the true anomaly of the cutoff point is found by

$$\phi = \phi_T + \alpha_D \tag{40}$$

and then R_T, V_T, and θ_T are determined by

$$R_T = \frac{P}{(1 + e\cos\phi)} \tag{41}$$

$$V_T = (\mu/P)^{1/2}\ (1 + 2e\cos\phi + e^2)^{1/2} \tag{42}$$

and

$$\theta_T = \tan^{-1}\ e\sin\phi/(1 + e\cos\phi)\ . \tag{43}$$

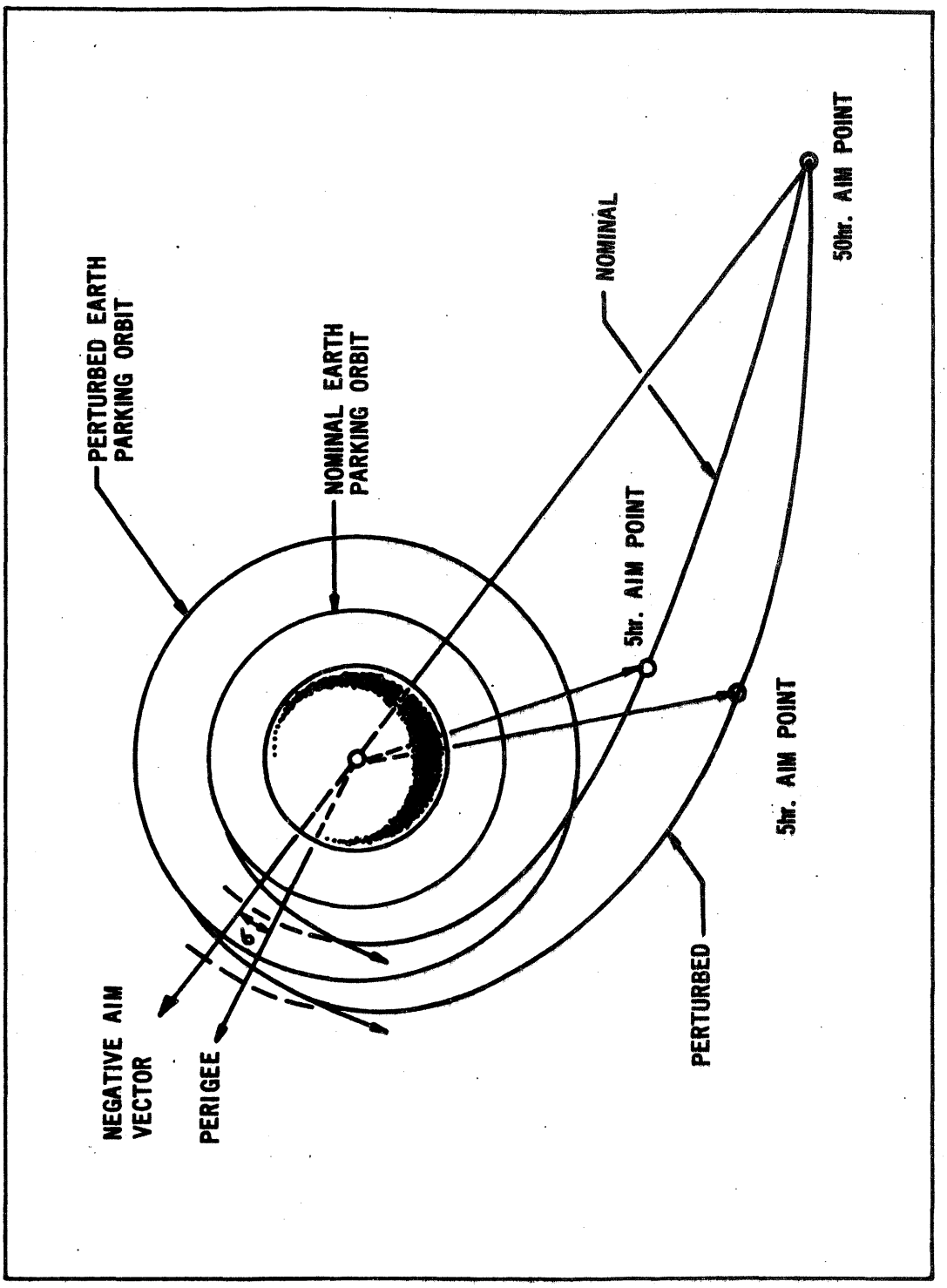

Figure 8. IN-PLANE PERTURBATION GEOMETRY

This completes the equations necessary to compute the five targeting parameters using the hypersurface. These equations are

$$(1)\quad R_T = \frac{P}{1 + e\cos\phi}$$

$$(2)\quad V_T = (\mu/P)^{1/2}\,(1 + 2e\cos\phi + e^2)^{1/2}$$

$$(3)\quad \theta_T = \tan^{-1} e\sin\phi/(1 + e\cos\phi)$$

$$(4)\quad i = \cos^{-1}(\vec{\Omega}_y \cdot \vec{N}_{PC})$$

$$(5)\quad \theta_N = \tan^{-1}\frac{(\vec{\Omega}_z \cdot \vec{F})}{(\vec{\Omega}_x \cdot \vec{F})}\ .$$

The development of the equations necessary to compute the targeting parameters for the three basic types of space missions has been presented. The equations have been programmed into a targeting subroutine and the results of runs for the various types of missions are presented in the next section. The logic flow for the subroutine as it is programmed is shown in Figure 9.

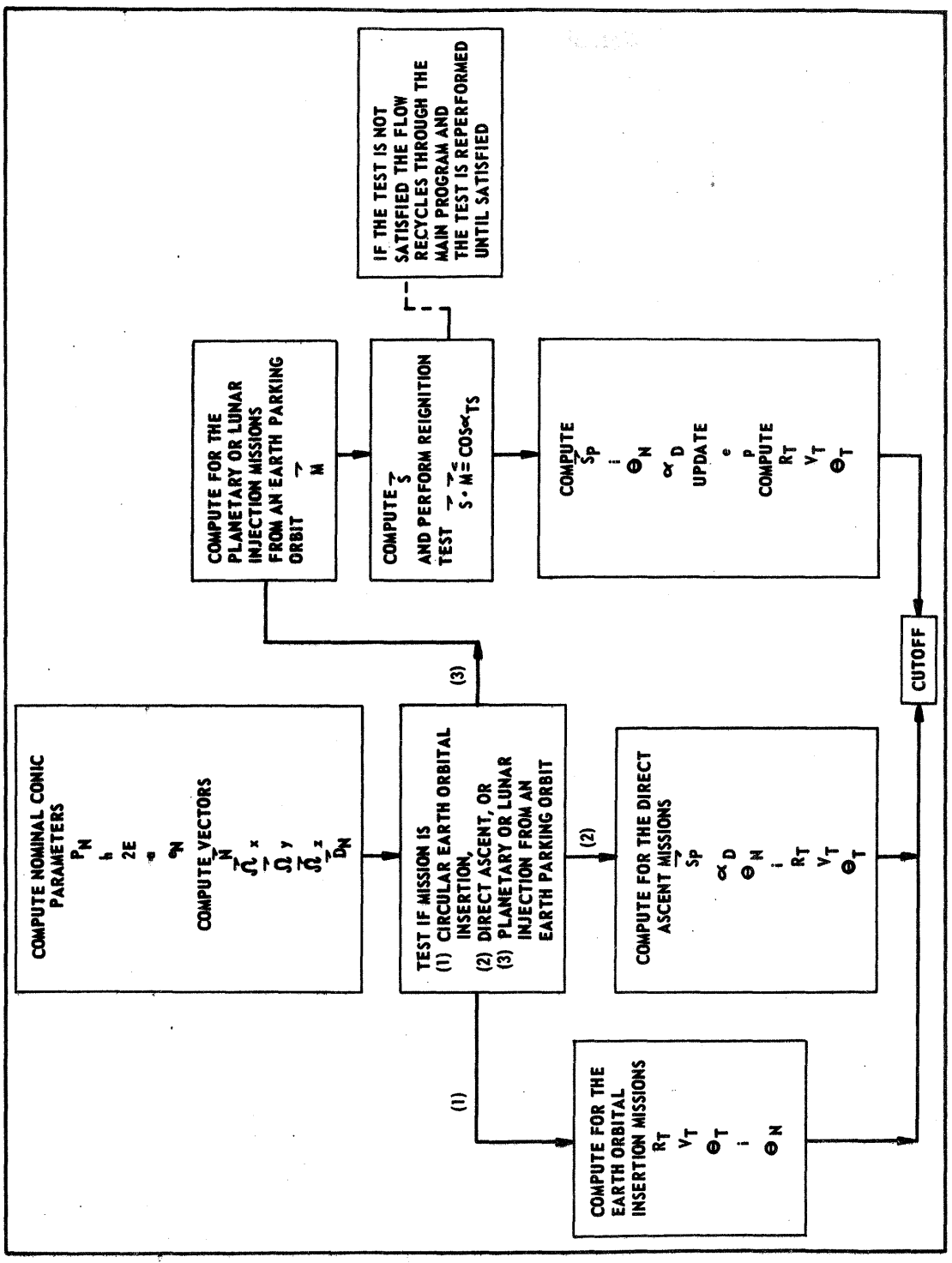

Figure 9. GENERALIZED TARGETING SUBROUTINE

CHAPTER IV

EXPERIMENTAL VERIFICATION

This chapter presents the results of several runs using the generalized targeting equations. The cutoff conditions for the three types of space missions previously mentioned are given as well as the arrival conditions for a Mars mission using the hypersurface.

A circular Earth orbital insertion mission was simulated from launch to insertion into the circular orbit with the following results:

Burn Time sec	Weight lb	Radius m	Velocity m/sec	Theta deg
687.907	274675.581	6563377.481	1793.753	-0.002

where the values given are for the circular orbit insertion point. These results are very close to the nominal values as R_T and V_T are exact, θ_T is off by .001 degree and the burn time is .001 second long. A direct ascent type mission (for a lunar trajectory) was also simulated with the following results:

Burn Time sec	Weight lb	Radius m	Velocity m/sec	Theta deg
1036.731	118900.377	6700333.291	10839.258	7.306

These results are with variable end conditions which one recalls will allow the true anomaly of cutoff to vary but the orientation of the conic remains fixed. This run was also made using fixed end conditions with the following results:

Burn Time sec	Weight lb	Radius m	Velocity m/sec	Theta deg
1037.152	118702.665	6688417.123	10849.391	7.028

The results of these two runs show that the variable and fixed end conditions cutoff (terminal) points are quite different. Even though the radius, velocity, and flight path angle at cutoff differ, both results will satisfy the mission requirements. It may be noted that for this trajectory the variable end condition case is optimum.

In order to show the effect of a velocity perturbation, a Mars mission was simulated in the following manner. It is assumed that 193 seconds after liftoff the vehicle has an error in the "y" component of velocity of $\pm$61 meters/sec. The mission is one in which the vehicle burns to an Earth circular parking orbit, then reignites and burns to injection into the planetary conic. The insertion into the circular orbit yields the following results:

Case	Radius/meters	Velocity/m/sec	Theta/deg	Weight/lb
Nominal	6559725.921	7796.004	.022	286431.074
$\dot{Y}$+61m/sec	6559725.793	7796.004	.022	286328.125
$\dot{Y}$-61m/sec	6559725.927	7796.005	.022	286300.462

which shows that a weight penalty has been added because of the perturbation but the accuracy of the cutoff conditions is still excellent. For each case the vehicle was then reignited and flown to injection into the planetary conic using the hypersurface with the following results:

Case	Radius/meters	Velocity/m/sec	Theta/deg	Weight/lb
Nominal	6782282.014	12251.345	10.309	92253.653
$\dot{Y}$+61m/sec	6782278.952	12251.348	10.308	92226.718
$\dot{Y}$-61m/sec	6782205.194	12251.399	10.307	92210.581

which shows that the total weight penalty is only 43 lb for the $\dot{Y}$-61m/sec case and only 27 lb for the $\dot{Y}$+61m/sec case. The cutoff conditions are also very good. This demonstrates the cutoff conditions for each of the three types of space missions given: circular Earth orbital insertion, direct ascent, and lunar or planetary injection from a circular parking orbit.

A Mars mission is now presented that demonstrates the accuracy of the arrival conditions at the desired target. The out of orbit phase of the mission which includes the burn from the parking orbit to planetary injection,then the free flight to the radius of closest approach (hereafter called RCA) at Mars is simulated. As stated in the discussion of the hypersurface,there are two empirically determined angles that are used in the hypersurface formulation:

(1) Sigma (σ) - The true anomaly of the negative aim vector

and

(2) Beta (β) - The angle from reignition to the intersection of the parking orbit plane and transfer conic plane.

An engineering experimental design approach that employs statistical analysis methods is used to demonstrate the effect of σ, β, and various parking orbit perturbations on the desired RCA at Mars. The mission employed is a Mars mission for 15 August 1973.

The response variable is the RCA at Mars and three independent variables are utilized: sigma, beta, and initial position. The angles

sigma and beta were chosen as independent variables because they are empirically determined quantities and their effect on various parking orbit perturbations is desired. In order to obtain meaningful results with statistical methods, a source of experimental error is needed.

To insure that some experimental error was inherent in the results, a Gaussian random number generator was used to vary the thrust and Isp of the S-IVB stage of the Saturn V within $\pm$ 3σ values. Other factors could have been employed as the independent variables as well as sources for the experimental error, but the choice depends on which factors the experimenter considers most important.

The levels of the independent variables were:

I. Position (P)

1. Y-100,000 meters
2. Y+100,000 meters
3. X+10,000 meters
4. X-10,000 meters

II. Sigma (S)

1. -45.6°
2. -39.6°
3. -33.6°
4. -27.6°

III. Beta (β)

1. 110°
2. 90°
3. 70°
4. 50°

No position perturbations in the Z directions were used as this perturbation should be eliminated by the reignition criteria. The experimental model is symmetrical and of the type

$$p = 3$$

$$k_1 = k_2 = k_3 = 4$$

$$N_s = N_f = k^p = 4^3 = 64$$

$$r = 2$$

$$N = r \cdot N_s = 2(64) = 128$$

where

p = number of independent variables

N_s = number of cells in the basic experiment

N_f = number of responses in the basic experiment

N = total number of responses in the experiment

k = number of levels for the independent variables

r = number of replications of the basic experiment.

The following effects are of interest:

P_i - main effect of position

S_j - main effect of sigma

S_l - linear effect of sigma

S_q - quadratic effect of sigma

S_c - cubic effect of sigma

β_k - main effect of beta

β_l - linear effect of beta

β_q - quadratic effect of beta

β_c - cubic effect of beta

PS_{ij} - interaction of position and sigma

$P\beta_{ik}$ - interaction of position and beta

$S\beta_{jk}$ - interaction of sigma and beta

The mathematical model is

$$R_{ijk} = \bar{y} + P_i + S_j + \beta_k + PS_{ij} + P\beta_{ik} + S\beta_{jk} + \varepsilon(ijk)$$

where R_{ijk} represents the measured variable, $\bar{y}$ represents a common effect in all observations (the true mean of the population from which all the data came), and P_i represents the position effect. S_j stands for the sigma effect and β_k represents the effect of the angle beta on the response variable R_{ijk}. $\varepsilon(ijk)$ represents the random error in the experiment. This error term is considered a normally and independently distributed random effect whose mean value is zero and whose variance is the same for all levels.

Since there were three independent variables with four levels for each of these variables, the basic experiment required 64 runs. However, because a Gaussian random number generator was used to vary the thrust and Isp, each of the 64 runs was replicated. This insured a better sample at each of the levels since a different Isp and thrust was used for each run. Consequently, the experiment required 128 runs to obtain the necessary data. The results of the 128 runs - the RCA at Mars for various sigma, beta, and position variations - are shown in the table on the following page. This table shows two values for the response variable, RCA, for each of the four levels of the independent variables. The values are given in kilometers (km). The nominal RCA value for this trajectory is 4994 km and was obtained from a calculus of variation run.

RCA AT MARS FOR VARIOUS BETA, SIGMA, AND POSITION VARIATIONS

		Position			
		Y-100	Y+100	X+10	X-10
β110	S-45.6	7807 7873	18383 18451	3923 3962	4076 4075
	-39.6	5609 5602	5193 5130	4968 4226	5065 5067
	-33.6	17114 17124	1439 1381	5896 5842	5824 5987
	-27.6	28053 28028	9262 9307	6631 6672	6573 6728
β90	S-45.6	4329 4288	4269 4187	4235 4251	4247 4393
	-39.6	5003 5042	5130 4206	4943 4892	5125 4976
	-33.6	5790 5811	5707 5687	5627 5574	5671 5637
	-27.6	6456 6466	6558 6321	6249 6291	6312 6337
β70	S-45.6	13372 13321	3208 3217	4247 4271	4460 4393
	-39.6	5051 5055	5262 5298	4789 4808	5020 4952
	-33.6	694 6992	5739 5841	5670 5517	5488 5478
	-27.6	6697 6618	6405 6316	6085 6250	6056 6079
β50	S-45.6	22331 22306	10146 10212	4752 4655	4562 4363
	-39.6	5275 5208	5703 5601	5047 5038	4973 4969
	-33.6	6999 6882	22869 22802	5395 5398	5915 4345
	-27.6	26661 26603	43987 43912	5859 5861	5913 5839

The following hypotheses were tested:

H_0: $P_i = 0$ for all i

H_1: $S_j = 0$ for all j

H_2: $S_1 = 0$

H_3: $S_q = 0$

H_4: $S_c = 0$

H_5: $\beta_k = 0$ for all k

H_6: $\beta_1 = 0$

H_7: $\beta_q = 0$

H_8: $\beta_c = 0$

H_9: $PS_{ij} = 0$ for all ij

H_{10}: $P\beta_{ik} = 0$ for all ik

H_{11}: $S\beta_{jk} = 0$ for all jk

Computations were made with the data and the results compiled in an ANOVA table.

ANOVA

SOURCE	DEGREES OF FREEDOM	SUM OF SQUARES	MEAN SQUARE	F CALCULATED	F TABLE
P_i	3	818,578,650	272,859,550	13.45	4.04
S_j	3	685,912,310	228,637,436	11.28	4.04
S_l	1	325,146,617	325,146,617	14.16	6.96
S_q	1	354,635,000	354,635,000	15.44	6.96
S_c	1	6,130,693	6,130,693	.267	6.96
β_k	3	801,171,320	267,057,106	13.17	4.04
β_l	1	148,125,895	148,125,895	6.45	6.96
β_q	1	646,763,080	646,763,080	28.16	6.96
β_c	1	6,282,345	6,282,345	.284	6.96
PS_{ij}	9	481,963,870	53,551,541	2.65	2.64
$P\beta_{ik}$	9	1,097,153,300	121,905,922	6.01	2.64
$S\beta_{jk}$	9	503,126,530	64,791,812	3.19	2.64
ϵ_{ijk}	91	1,844,950,320	20,274,179		
TOTAL	127	6,312,856,300			

The F calculated column is the ratio of the variance of a particular factor and the experimental error factor. The F table column is the acceptable F value for particular degrees of freedom at a 95-percent significant level. The results indicate that all the main effects and the interactions are significant, therefore the hypothesis H_0, H_1, H_5, H_9, H_{10}, and H_{11} can be rejected. Also, sigma has definite linear and/or quadratic trends while beta has definite quadratic trends. Since the effects of each of the main factors are significant, this indicates there is a considerable difference in the average values for each level of these factors. The F test on the interactions is also significant which implies there is interaction between each of the three factors.

The results indicate that the values of sigma and beta have a definite effect on the desired end conditions (RCA). A sigma value of -39.6° and beta of 90° yields the closest RCA to the nominal for all the position perturbations. This value of sigma is as expected since this positions the aim vector parallel to the outgoing asymptote of the hyperbolic conic.

The following table presents the variation of the RCA for the nominal ignition point and for the previously given initial position perturbations. The thrust and Isp were varied exactly ± 3 percent for these runs, whereas previously, the variation was within $\pm 3\sigma$ as determined by a random number generator. These runs were made with $\sigma = -39.6°$ and $\beta = 90°$. The accuracy obtained is well within the limits needed.

ΔRCA AT MARS FOR VARIOUS POSITION AND PERFORMANCE PERTURBATIONS

POSITION PERTURBATION	PERFORMANCE PERTURBATION	ΔRCA VARIATION/km
Nominal	Thrust ± 3%	-180 to 293
	Isp ± 3%	-62 to 138
X + 10 km	Thrust ± 3%	-283 to 186
	Isp ± 3%	-165 to 44
X - 10 km	Thrust ± 3%	-292 to 200
	Isp ± 3%	-148 to 52
Y + 100 km	Thrust ± 3%	-240 to 242
	Isp ± 3%	-118 to 92
Y - 100 km	Thrust ± 3%	-27 to 262
	Isp ± 3%	-93 to 117

CHAPTER V

CONCLUSIONS

This thesis has presented the development of the equations necessary to compute the targeting parameters for the iterative guidance mode. The results of using these equations have yielded excellent injection conditions for all types of space missions. The arrival conditions for an interplanetary mission to Mars also demonstrated very good accuracy with the use of these equations. Thus, the validity of the equations developed has been firmly established.

BIBLIOGRAPHY

Books

1. Bartee, E. M., Statistical Methods in Engineering Experiments, Columbus, Ohio, Charles E. Merrill Books, Inc., 1966.

2. Dixon, W. J., and Massey, F. J., Introduction to Statistical Analysis, Second Edition, New York, McGraw-Hill Book Company, Inc., 1957.

3. Hicks, Charles P., Fundamental Concepts in the Design of Experiments, New York, Holt, Rinehart, and Winston, Inc., 1964.

4. Nelson, W. C. and Loft, E. E., Space Mechanics, Englewood Cliffs, N.J., Prentice Hall, Inc., 1962.

Reports

5. Deaton, A. W., "Saturn V Translunar Injection Guidance System," Presentation to Dr. von Braun, George C. Marshall Space Flight Center, Huntsville, Alabama, 7 April 1967.

6. Horn, H. J., Martin, D. T., and Chandler, D. C., "An Iterative Guidance Scheme and its Application to Lunar Landing," MTP-AERO-63-11, George C. Marshall Space Flight Center, Huntsville, Alabama, 6 February 1963.

7. Lawden, D. F., "Optimal Rocket Trajectories," Jet Propulsion, Vol. 27, December 1957.

8. Martin, D. T. and Hooper, H. L., "A Simplified Cutoff Hypersurface for Iterative Guidance during the Lunar Injection Burn," NASA TMX-53025, George C. Marshall Space Flight Center, Huntsville, Alabama, 17 March 1964.

9. McCraney, R. M., "Generalized Hypersurface Subroutine," Northrop Technical Memorandum No. 297, Northrop Space Laboratories, Huntsville, Alabama, November 1966.

10. Smith, I. E., "General Formulation of the Iterative Guidance Mode," NASA TMX-53414, George C. Marshall Space Flight Center, Huntsville, Alabama, 22 March 1966.

11. Smith, I. E., and Cooper, D. F., "Launch Vehicle Guidance Equations for the Saturn IB SA-201 Mission," NASA TMX-53215, George C. Marshall Space Flight Center, Huntsville, Alabama, 12 March 1965.

12. Tucker, W. B., Hooper, H. L., and Lester, R. C., "Function Yielding Earth Departure and Lunar Arrival Conditions," R-AERO-IN-12-64, George C. Marshall Space Flight Center, Huntsville, Alabama, 22 May 1964.

13. -----, The Boeing Company, "Saturn V Launch Vehicle Guidance and Navigation Equations, SA-504," Document No. D5-15429-4, 12 October 1966.

14. -----, The Boeing Company, "Explanation of SA-501 Reignition and Targeting Geometry," 30 December 1965.